Edge-on disk galaxies

Grijs, Richard de

Chapter 3

The vertical stellar distribution in NGC 6504 – detection of a thick disk

Abstract. The vertical stellar distribution of the edge-on spiral NGC 6504 is examined in seven bands (*U, B, R, I, J, H, K*) by fitting model distributions to the light profiles at seven positions along the major axis. In the inner parts of the disk the profile is well approximated by an exponential distribution. At large galactocentric distances, the profile is much less steep near the equatorial plane, being fitted better by, e.g., a sech(z) distribution. We find an excess of light at large z values, in all optical bands and at all radii. We confirm the constancy of the scale height as a function of radius. Our best explanation for the deviations from the sech(z) distribution at small z is dust extinction in combination with a young disk component. This young disk component has a very small scale height (it is unresolved) and a smaller scale length than that of the (thin) disk. The excess at large z can be modeled by a component that looks very much like the thick disk in the Galaxy: scale height $\sim$ 4 times the scale height of the thin disk, and central surface brightness $\sim$ 1% of the brightness of the thin disk.

1 Introduction

The stellar distribution in galaxies provides valuable information about the gravitational potential and gives insight into the various stellar populations of which galaxies are composed.

In spiral galaxies, one often distinguishes the disk, the bulge and the halo. In our Galaxy, we also differentiate between a young, a thin and a thick disk. Because of their large distances, studying disks of edge-on galaxies in the same detail as for our Galaxy is impossible, and very few studies have been undertaken to establish the existence of young and thick disks in external galaxies. Even so, this information is fundamental to understand the early evolution and present star formation activity of spiral galaxies.

This Chapter reports on the analysis of surface brightness profiles perpendicular to the plane in the edge-on galaxy NGC 6504. We investigate the shape of the vertical stellar distribution, on the basis of optical images in 4 different bands. In Sect. 5, we present evidence for a thick disk in this galaxy.

1.1 Galaxy components

To avoid confusion about terminology, we will briefly discuss the components that we take to be contributors to the light distribution in spiral galaxies.

The most prominent stellar components in most spiral galaxies are the thin (or old) disk and the bulge. The scale height of the thin disk in our Galaxy is in the range 150 – 300 pc (Sandage, 1987; Kent et al., 1991). Apart from these, several other stellar components have been described: the young disk, the thick disk and the halo.

The young disk is a region of active star formation very close to the disk midplane. The young disk has been detected in a few disk galaxies, e.g. NGC 4452, NGC 4762 (Hamabe & Wakamatsu, 1989) and NGC 4565 (Jensen & Thuan, 1982). Hamabe & Wakamatsu derive a scale height of $\sim$ 100 pc. The young disk is unresolved in NGC 4565. Detection is hard, because dust obscuration plays a major role at small z.

The term thick disk refers to a flattened component with scale height of order 1 kpc. In the Galaxy its presence is derived from star counts above the plane of the Galaxy in the solar neighbourhood (Gilmore & Reid, 1983; Sandage, 1987; Sandage & Fouts, 1987). Its stellar population is predominantly old. It is uncertain whether the thick disk and the thin disk are two distinct components or if a continuum exists in velocity dispersion, metallicity and age between the thin disk and the thick disk (Carney et al., 1989). Since the work of Tsikoudi (1979) and Burstein (1979) it seems that thick disks are quite common in S0 galaxies. The existence of a thick disk in spiral galaxies other than our own is subject of ongoing debate. We will discuss this in more detail in Sect. 5.1.

The halo consists mainly of globular clusters and old stars (Sandage & Fouts, 1987). Its scale height in the solar neighbourhood is $\sim$ 3.2 kpc (Sandage, 1987). The surface brightness of the halo is very low compared to that of the thin disk. It will not be considered further in this Chapter.

1.2 Vertical distributions

Up to now three different functions have been used to describe the vertical light distribution of spiral galaxies. If the disk of a spiral galaxy can be approximated by an isothermal sheet the density is given by

$$\rho(z) = \frac{\langle W^2 \rangle}{2\pi G {z_0}^2} \,\mathrm{sech}^2\left(\frac{z}{z_0}\right) \quad , \tag{1}$$

where W is the vertical velocity, z the distance from the plane and z_0 the scale height. If we assume a constant mass-to-light ratio, M/L, then the light distribution also has a sech$^2(z)$ dependence.

This function was successfully used by van der Kruit & Searle (1981a, 1981b) for the modeling of NGC 4244, NGC 5907 and NGC 891. However, Aoki et al. (1991) find that, in the near infrared, the vertical light distribution of NGC 891 is best fitted by an exponential function, which is steeper than sech^2 towards the equatorial plane. They argue that extinction by dust is probably the cause for the flattening of the verti-

A slightly modified version of this Chapter was published as *van Dokkum, P.G., Peletier, R.F., de Grijs, R., Balcells, M., 1994, A&A 286, 415*

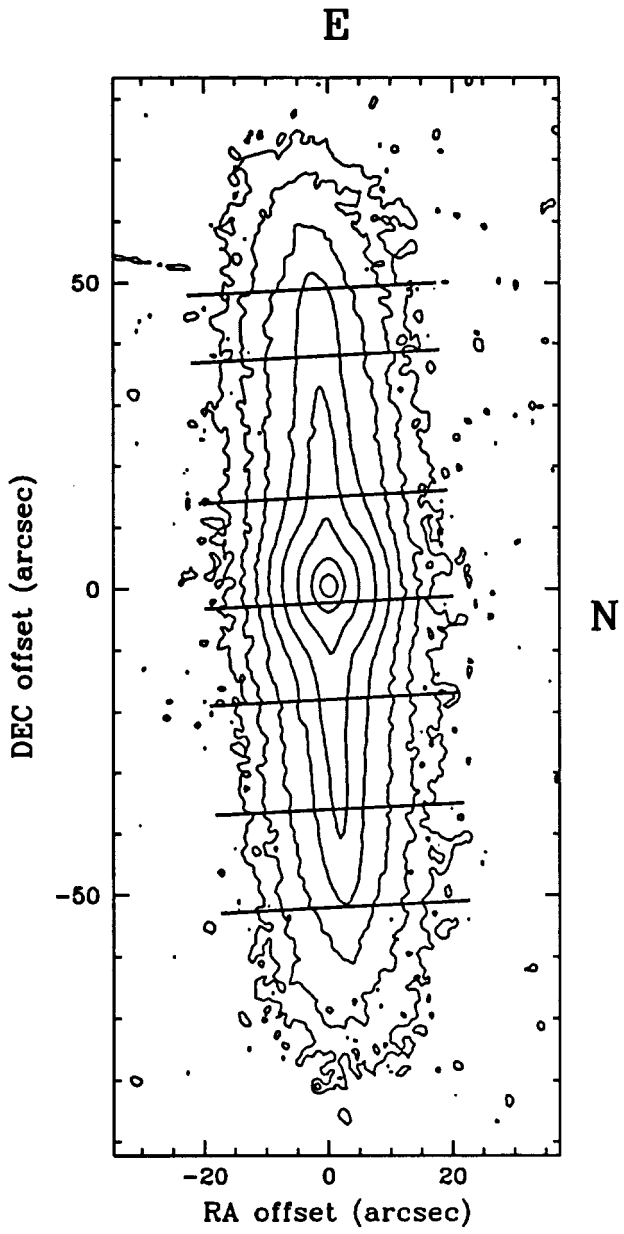

Fig. 1. *I*-band contour plot of NGC 6504. The lowest contour is 24 mag arcsec^{-2} and the highest 17 mag arcsec^{-2}. The interval between successive contours is 1 mag arcsec^{-2}. The lines show the positions at which profiles were extracted. East is up and north is to the right.

cal surface brightness profiles towards the equatorial plane of NGC 891 in the optical.

Using star counts of the Galaxy, Gilmore & Reid (1983), as well as Pritchet (1983), concluded that the vertical stellar distribution in our Galaxy is exponential. This result was confirmed by Kent et al. (1991) who studied images obtained with the *Infrared Telescope* (flown aboard the Space Shuttle in 1985 as part of the *Spacelab 2* mission).

A third function, proposed by van der Kruit (1988), is the sech(z) function, a compromise between the sech^2 and the exponential. As is the case for the exponential distribution, there is no direct physical explanation for it. This function was adopted by Barnaby & Thronson (1992) for their H band model of NGC 5907 and it fitted the data rather well.

The three functions have been fitted successfully in the past, so the question is not which function can be used best to fit the vertical surface brightness profiles in B or V, but what function best approximates the distribution of the stellar light after the effects of dust extinction have been taken into account. Is the stellar light distribution exponential, as it seems from the near infrared (NIR), or are there cases where a sech(z) or a sech^2(z) fits better, even after correction for extinction? Or does one need a distribution which is even steeper than exponential in the centre?
We decided to take a large, extremely edge-on galaxy, chosen randomly, to investigate these questions.

2 Observations and reduction

NGC 6504 ($\alpha\,(2000) = 17^{\rm h}56^{\rm m}6^{\rm s}$; $\delta\,(2000) = 33^\circ 12' 36''$) is of morphological type S (RC3; de Vaucouleurs et al., 1994). The regular structure and the smooth spectrum of the galaxy suggest that NGC 6504 is not a late type galaxy. On the basis of its dustiness (Sect. 3) we would classify it as Sab.

2.1 Observations

Imaging CCD observations in U, B, R and I were obtained with the 2.5m Isaac Newton Telescope (INT) at La Palma, Spain on June 18, 1990. The integration times in U, B and R were 1200, 600 and 60 seconds, respectively. We retrieved additional I band observations from the La Palma archive (observations with the same setup by Florido et al., 1991), resulting in a total I band integration time of 300 seconds. The pixel size of the frames was $0\farcs549$. Details of the observations and reductions can be found in Balcells & Peletier (1994).

NIR images in J, H and K were obtained at Kitt Peak National Observatory on October 5, 1990 with the 2.1m telescope, equipped with IRIM and a 62×58 InSb detector. The integration times were 2×100 seconds in J and H and $2 \times 3 \times 60$ seconds in K. The pixel size was $0\farcs514$ in J and H and $0\farcs511$ in K.

We measured the heliocentric redshift of NGC 6504 in service time on the INT in September 1993. It proved to be 4970 ± 20 km s^{-1} which implies a distance of 66 Mpc, for a Hubble constant $\rm H_0 = 75\ km\,s^{-1}Mpc^{-1}$, which we will use throughout this Chapter. On this scale $1''$ equals 320 pc.

2.2 Data reduction

The standard photometric reduction was applied to the optical data. After bias subtraction and flatfielding all 'visible' point sources were removed by interpolating the area around them. Then a small gradient across the frame (a difference of $\sim 1\%$ of the sky value between both sides of the frame) was removed by fitting a one-dimensional polynomial to regions far away from the galaxy. At the same time this took care of the sky subtraction. The remaining background variations are statistical, so that our uncertainties are mainly due to Poisson noise. The effective seeing measured from stars was $1\farcs6$ in U and B, $1\farcs3$ in R and $1\farcs2$ in I.

In the NIR the effective seeing was $\sim 1\farcs2$. Here the galaxy was moved around on the chip in between observations, to

obtain better flatfielding. The reduction procedure of the NIR data can be found in Peletier (1993).

2.3 Analysis

Vertical profiles were extracted at seven positions along the major axis of the galaxy. To improve the signal-to-noise ratio we binned the data in the radial and vertical direction. The 'central' profile was taken 2.″2 west of the true centre, because the central profile was affected by a bright foreground star. The positions where profiles were extracted as well as the widths of the radial bins are given in Table 1. In Fig. 1 a contour plot of NGC 6504 is shown.

Table 1. Positions along the major axis at which profiles were extracted.

nr.	position	width
1	52″ (16.6 kpc) W	5.″5
2	36″ (11.5 kpc) W	5.″5
3	18″ (5.8 kpc) W	2.″7
C	2.″2 (0.70 kpc) W	1.″7
4	15″ (4.8 kpc) E	2.″7
5	38″ (12.2 kpc) E	5.″5
6	49″ (15.7 kpc) E	5.″5

In the NIR (J, H and K) only one profile was made (at 2.″2 W) because of the small field of view of the array. In Fig. 2 we present the I-band profiles at each of the numbered positions.

3 Modeling

The aim of our modeling is to describe the vertical stellar profiles. Therefore the model is allowed to differ from the light distribution in some areas as long as a reasonable explanation can be found for the deviations (dust extinction, for example). We will first describe an exponential model. On the basis of deviations from this model we will subsequently fit different, non-exponential distributions.

3.1 Exponential model

3.1.1 First model: fit to all points

The model we tried first is a simple exponential function, fitted to all points with $|z| < 40''$ (12.8 kpc). Figs. 3 (a) and (b) show the residuals obtained by subtracting this model from two typical profiles. Table 2 gives the parameters of the fits. In Figs. 4 (a) and (b) the exponential scale height as a function of radial distance is shown.

This model fits the data very well. However, as we notice in Fig. 4, the scale height is larger at shorter wavelengths, contrary to results from our Galaxy. This is probably caused by dust: the extinction is highest near the galactic plane and dust is more important at shorter wavelengths. The effect of dust would be that the U and B profiles are depressed in their inner regions, so that a fit using all points would result in a larger scale height. Since we do not have any other physical explanation, we argue that the deviations are caused by dust extinction. Consequently, we try to minimize the influence of dust on the fits in a second model.

All profiles can be approximated well by an exponential function between $|z| = 10''$ and $|z| = 16''$. At larger z, fluctuations due to the low signal-to-noise ratio may affect the profiles, whereas the central dip, which is seen in some profiles, is excluded by the lower limit of $10''$.

3.1.2 Second model: fit to linear part of profiles

The second model therefore is a fit to the region $10'' \leq |z| \leq 16''$. The residuals of the fits are shown in Figs. 3 (c) and (d). The fit parameters are given in Table 2 and plotted in Figs. 4 (c) and (d).

Figure 4 (c) and (d) show that the scale height no longer exhibits a dependence on radius. Furthermore the scale height in the I band appears to be constant with radius ($\langle z_0 \rangle = 3.''34 \pm 0.''12$). The large scatter in the U band (and also, but smaller, in B) is presumably caused by dust and star formation. Both these effects are more prominent at shorter wavelengths. The irregularities in U are also partly due to the low signal-to-noise ratio in this band.

Since the scale height variations as a function of passband are small and appear to be random, we assume that they are caused by patchy dust extinction and statistical errors. In the I band the influence of dust is very small and the signal-to-noise ratio high, so in the next model the profiles in this band are taken to represent the best approximation to the true (dust-free) distribution of the older stellar population.

3.1.3 Third model: second model, with fixed scale heights

The third model is based on the following assumptions:

1. The scale height of the (old) stellar distribution is equal to the scale height in I in all bands.
2. Data at $|z| < 10''$ are (heavily) affected by dust.
3. At large $|z|$ (from $\sim 20''$ upwards) the profile is noisy, largely or entirely due to statistical fluctuations.

This model is therefore equal to the second model, but with the scale heights in all bands fixed to the scale height in the I band. The fits are shown in Figs. 3 (g) and (h). The residuals are shown in Figs. 3 (e) and (f). The parameters can be found in Table 2.

3.2 Deviations from the exponential model

In this section, we examine the deviations from the third exponential model. We distinguish between deviations in the outer parts (at large z) and in the inner parts (at small z).

3.2.1 Deviations at large z

In the outer parts an excess is seen in the profiles (Fig. 3). In order to examine whether this excess is real we consider three other possibilities:

Statistical fluctuations We have investigated the probability that the excess is caused by statistical fluctuations if the true profile is exponential. The residual after subtraction of the model is calculated in the I band (Table 3), averaging all points between $|z| = 20''$ and $|z| = 40''$.

We find a mean excess $\langle I_{\rm d} \rangle = 0.84$ with standard deviation 0.57. The probability that the excess in all profiles is zero is given by:

$$P(x \geq N\langle I_{\rm d} \rangle \mid \mu = 0 \mid \sigma_2 = \sqrt{N}\sigma_1), \qquad (2)$$

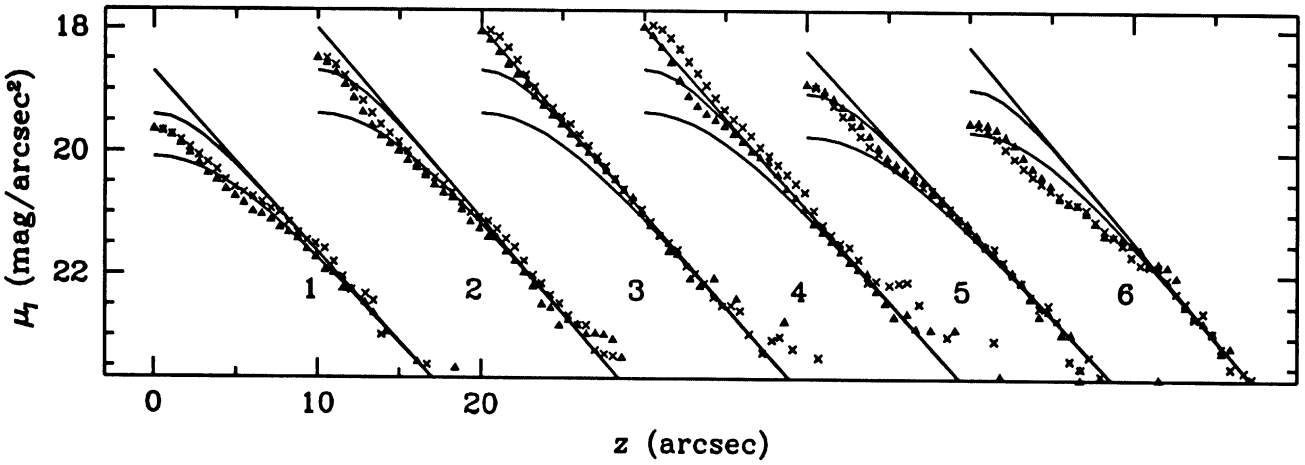

Fig. 2. Disk profiles in the I band, together with best fitting exponential (upper line), sech (middle line) and sech^2 functions (lower line). From left to right the profiles at 52″ W (1), 36″ W (2), 18″ W (3), 15″ E (4), 38″ E (5) and 49″ E (6) are shown. Triangles indicate the southern side, crosses the northern side.

Table 2. Exponential scale heights (in arcsec) of models 1 and 2.
The scale heights of model 3 are equal to the I-band scale heights of model 2.

pos	model 1 (I)	model 2 (I)	model 1 (R)	model 2 (R)	model 1 (B)	model 2 (B)	model 1 (U)	model 2 (U)
52″ W	4.54 ± 0.07	3.41 ± 0.08	4.55 ± 0.20	4.44 ± 0.64	4.39 ± 0.12	3.60 ± 0.24	3.86 ± 0.18	4.3 ± 1.5
36″ W	3.71 ± 0.03	3.24 ± 0.07	3.97 ± 0.06	3.83 ± 0.09	3.66 ± 0.05	3.57 ± 0.16	4.14 ± 0.10	4.00 ± 0.42
18″ W	3.37 ± 0.03	3.32 ± 0.03	3.53 ± 0.04	3.39 ± 0.06	3.83 ± 0.09	3.86 ± 0.09	4.42 ± 0.08	4.49 ± 0.24
2″.2 W	2.45 ± 0.02	2.33 ± 0.04	2.44 ± 0.02	2.23 ± 0.08	2.84 ± 0.03	2.50 ± 0.07	3.24 ± 0.04	2.52 ± 0.11
15″ E	3.49 ± 0.04	3.38 ± 0.09	3.60 ± 0.13	3.61 ± 0.08	3.95 ± 0.07	3.66 ± 0.06	4.34 ± 0.09	3.61 ± 0.10
38″ E	3.96 ± 0.09	3.49 ± 0.10	3.91 ± 0.06	3.02 ± 0.12	4.45 ± 0.07	3.71 ± 0.23	4.80 ± 0.15	2.76 ± 0.37
49″ E	4.16 ± 0.08	3.17 ± 0.06	4.18 ± 0.06	3.54 ± 0.17	4.22 ± 0.08	3.21 ± 0.16	5.08 ± 0.27	4.8 ± 1.5

Table 3. Excess in outer parts on south and north side (in instrumental I counts).

position	$I_{\rm data} - I_{\rm fit}$ (S)	$I_{\rm data} - I_{\rm fit}$ (N)
52″ W	0.00 ± 0.07	2.5 ± 1.0
36″ W	−0.2 ± 0.7	3.0 ± 0.6
18″ W	4.4 ± 0.7	0.1 ± 1.6
2″ W	0 ± 3	5 ± 2
15″ E	2 ± 3	4.1 ± 1.6
38″ E	0.9 ± 1.4	3.7 ± 1.1
49″ E	−0.06 ± 0.19	2.1 ± 0.6

where N is twice the number of profiles (14), σ_1 is the standard deviation of the average intensity difference (0.57) and x has a Gaussian distribution with average μ and standard deviation σ_2. This leads to a probability of $P(\mu = 0) \ll 10^{-4}$. So, although the excess in the outer parts is not seen in every profile it cannot be attributed to statistical fluctuations.

Non-zero background level If the background is not subtracted correctly, a systematic excess may occur in the outer regions where the light contribution of the galaxy is low. The fact that our profiles are, on the average, symmetric shows there is no gradient in the background. In the I band, the uncertainty in the subtraction of the sky background is $\sigma = 1.1$ counts, or 0.37% of the background level, as determined from the mean levels in various boxes in the frame. We examined the effect of a systematic error in the subtraction of the background on the average I-band profile (Sect. 5.2) by adding and subtracting σ and 2σ. From Fig. 5 it is clear the excess at large radii cannot be created by a wrongly subtracted background.

Instrumental scattering Another possible explanation for the excess is instrumental scattering. Smoothed light from the bright central regions might cause artifacts at large z. From the investigation of the profile of a star of the same brightness as the central regions of NGC 6504, we find that at distances of more than 20″ the scattered light of the bright inner regions is negligible compared to the light of the galaxy.

3.2.2 Deviations near the plane

At small heights the profiles show the following features:

1. An overall intensity dip, i.e. there is less signal than one would expect from an exponential fit between 10″ and 16″.
2. A small excess close to $z = 0$.
3. A minor dip on the north side (between $z = 0$ and $z = 5$″).

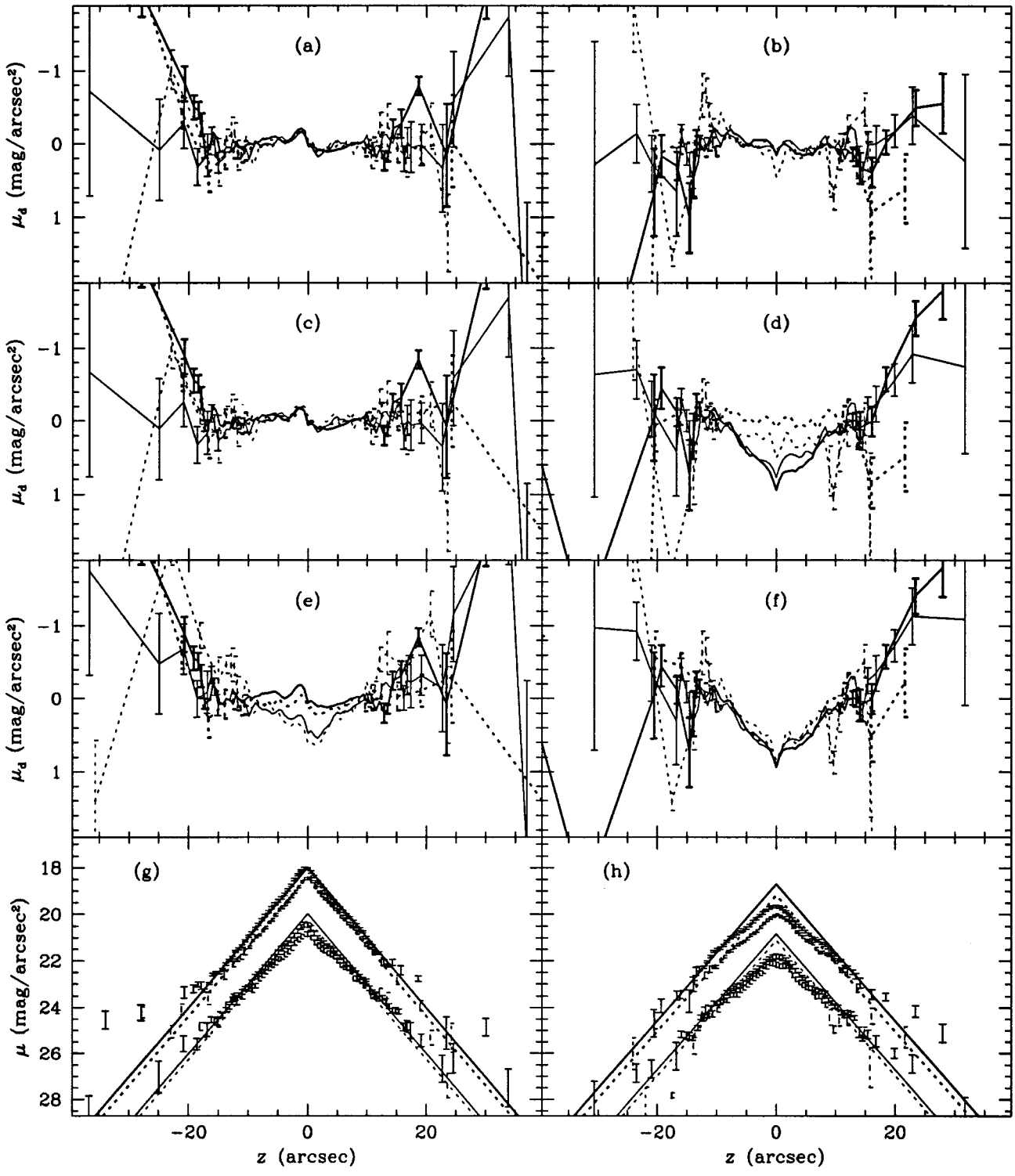

Fig. 3. Deviations from the exponential model. In the left panels the profiles at 18″ W (3) are shown, the right panels show the profiles at 52″ W (1). Here, (a) and (b) show the residuals after subtracting model 1, (c) and (d) the residuals of model 2 and (e) and (f) the residuals of model 3. The lines in (g) and (h) represent model 3. Bold solid lines represent I, bold dashed lines R, solid lines B and dashed lines U. Our binning algorithm was such that the mean values as well as the average positions are intensity weighted. The error bars associated with the binned intensities are 1σ errors.

The last two features are most prominent at small galactocentric radii. In Fig. 6 the average magnitude of the difference between data and fit is plotted against the radial distance from the centre (in the I band). The figure clearly shows that the deviations from the exponential model increase with radius.

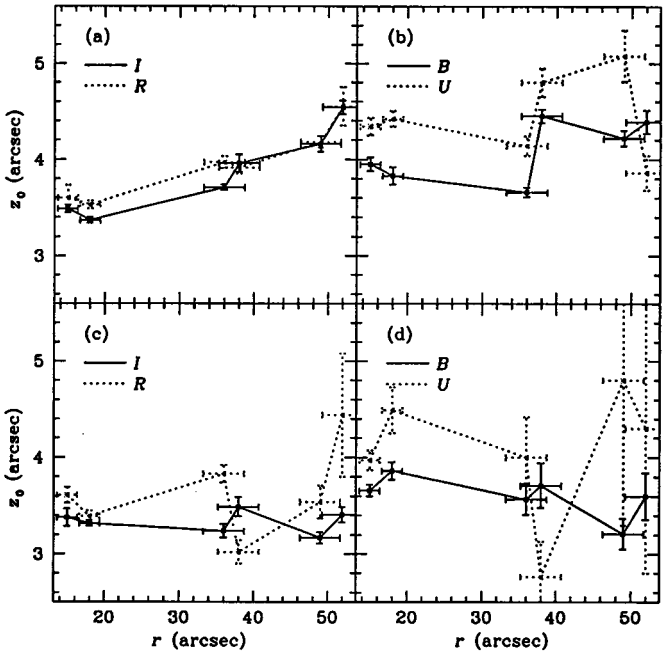

Fig. 4. Dependence of scale height on radius. (a) I (solid) and R (dashed) model 1, (b) B (solid) and U (dashed) model 1, (c) I and R model 2 and (d) B and U model 2.

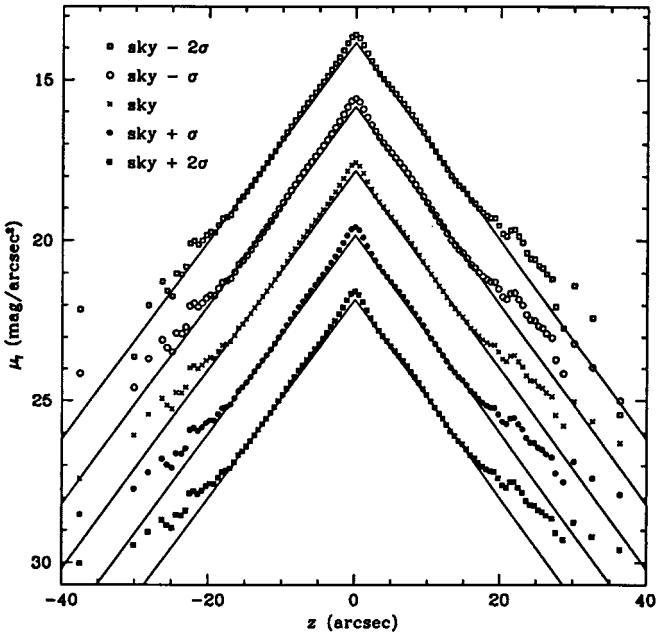

Fig. 5. Effect of a non-zero background on the average I-band profile of NGC 6504. The uncertainty in the background subtraction is $\sigma = 0.37\%$ of the background level (Sect. 3.2.1). The points represent the data with, from top to bottom, background $- 2\sigma$, background $- \sigma$, background, background $+ \sigma$, and background $+ 2\sigma$. The lines represent the third exponential model. Except for the middle profile the profiles have been displaced vertically for clarity.

3.3 Non-exponential distribution

Since the profiles at large radial distances from the centre of the galaxy show a clear deficit compared to the third exponential model we have fitted a sech(z) and sech$^2(z)$ law to the profiles as a fourth model.

Since Eq. (1) can be approximated by

$$\mathrm{sech}^2\left(\frac{z}{z_0}\right) \approx 4 \exp\left(-\frac{2z}{z_0}\right) \qquad (z \gg z_0) \tag{3}$$

the scale height of a sech$^2(z)$ fit, as well as that of a sech(z) fit that agrees with the exponential fit in the outer parts, can be calculated from the exponential scale height of our model. Figure 2 shows the exponential as well as the sech(z) and sech$^2(z)$ fitted to the profile in the I band at 6 positions along the major axis.

The exponential distribution is the best fit to most profiles of this galaxy. In the inner-disk profiles the data show a large excess over the sech(z) distribution. But going to the outer parts the fit to the sech(z) distribution gradually improves. The sech$^2(z)$ is only capable of describing the observations in the outermost profiles (52″ W (1) and 49″ E (6)).

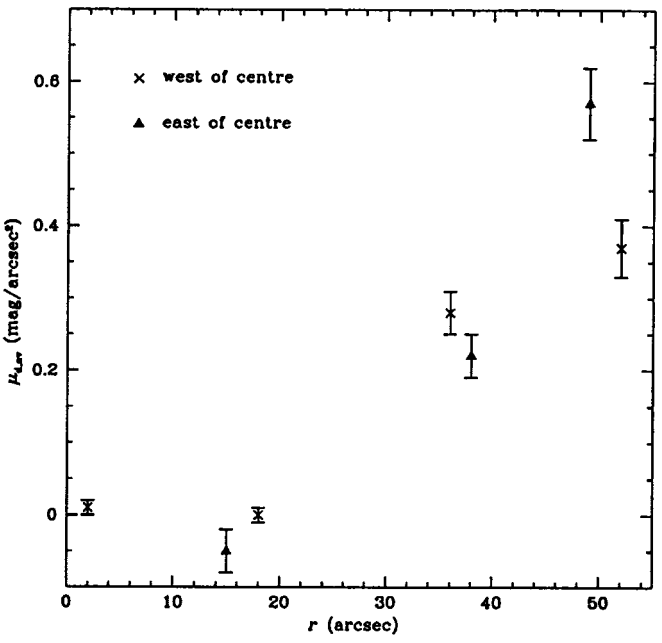

Fig. 6. Difference between the third exponential model and data in the inner parts of the I-band profiles.

3.4 Bulge model

In order to investigate the influence of the bulge on the disk profiles we examined its stellar distribution. In Fig. 7 the profiles in the 4 optical bands are shown.

The bulge is clearly exponential in I and R. Dust obscuration is probably the cause for the depressed inner parts in the B and U profiles.

We have made a model for the bulge following the procedure of Kent (1985). In this model, the fixed axial ratio of the bulge is 0.7, the position angle 93°, the central surface brightness 2.16 I mag brighter than the disk and the scale length $h_{\rm maj} = 2.31''$. These parameters imply that the surface brightness of the bulge at $15''$ E and $z = 0$ is 5 mag fainter than the surface brightness of the disk, which means that the influence of the bulge is already negligible at this position. After subtracting the bulge we find a central scale height of the disk of $2\farcs8$, comparable to $3\farcs3$, reached farther out.

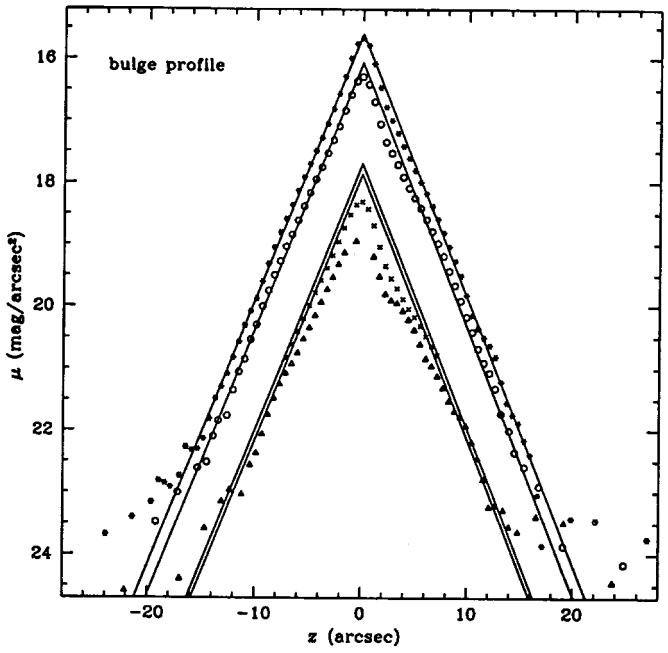

Fig. 7. Bulge profiles ($2\farcs2$ W) of NGC 6504. Triangles indicate U, crosses B, circles R and stars I. The scale height of the fits is taken equal to the scale height in the I band. Positive values of z indicate the north side, negative values the south side of the profiles.

4 Discussion

In the previous section we have analysed several model fits to the data. In this section we will try to explain what we found.

4.1 Inner parts

The deviations are listed in Sect. 3.2.2.

1. The excess at very small z suggests the presence of a young disk component. The scale height cannot be determined, since the young disk in unresolved. In comparison, the young disk in our Galaxy has a scale height of $\sim$ 100 pc, or $0\farcs3$ at the distance of NGC 6504.
The young disk shows up in all bands due to a combination of two effects: young stars radiate predominantly in blue but the extinction by dust is also highest in this band.

2. From the behaviour of the narrow intensity dip on the north side, especially in U and B, we conclude that it is caused by a pronounced dust layer. This implies that the galaxy is somewhat inclined; the northern side is the nearer side. Since the dust lane is not resolved the inclination cannot be measured exactly. From the fact that the dust lane is very close to the equatorial plane we estimate that the inclination is greater than 85°.

3. In Fig. 8 vertical colour profiles are shown at four positions along the major axis of the galaxy. The uniformity of the colour profiles outside the central regions shows that the dust is probably concentrated towards the centre, and is not distributed in a ring. Furthermore, the amount of extinction in the equatorial plane is not more than 1 mag arcsec^{-2} in B. Therefore, the flattening of the vertical profiles at $r \geq 36''$ cannot be caused by extinction, so that the surface brightness profile of the *stars* is not fitted well by an exponential, but rather by a sech(z) or sech^2(z) distribution. In the centre the presence of dust and probably a young disk make it very hard to say anything about the vertical profile of the stars near the equatorial plane.

It seems that the only consistent explanation here is that the young disk component has a smaller scale length than the disk component that provides most of the light (the thin disk). The vertical distribution of the thin disk is probably closer to sech(z) (as seen at large radii), and so it is the combination of the stars and dust in the young disk and the thin disk that gives rise to the exponential light profile in the centre.

The way to check this hypothesis is to obtain deep NIR profiles or to investigate other, similar galaxies (see, e.g., de Grijs et al., 1997 [Chapter 8]).

4.2 Outer parts

We have shown that the excess at large z heights is real. Now we will discuss some explanations.

A possibility is a $z^{\frac{1}{4}}$ behaviour of the bulge. At intermediate heights the disk is more prominent than the bulge, but at both small and large z a $z^{\frac{1}{4}}$ bulge would be more important than the disk. It is necessary that the bulge gets flatter towards the outer parts in that case. In the case of NGC 891, for example, the excess at large z found by van der Kruit & Searle (1981b) is thus explained by van der Kruit (1984).

For NGC 6504 this explanation is not likely. First of all, the bulge of NGC 6504 is small, with a scale height that is smaller by a factor of 2 than the scale height of the disk, which is in contradiction with the fact that the excess is also seen at large radii. Secondly, the bulge profile ($2\farcs2$ W) does not show any signs of a $z^{\frac{1}{4}}$ behaviour, but rather of an exponential dependence on radius.

Bahcall & Kylafis (1985) discuss another possible explanation for the excess in NGC 891: a thick disk component. They cannot decide between a thick disk and a "returning" $z^{\frac{1}{4}}$ bulge; both fits are quite good. In the next section the thick disk option for NGC 6504 is examined.

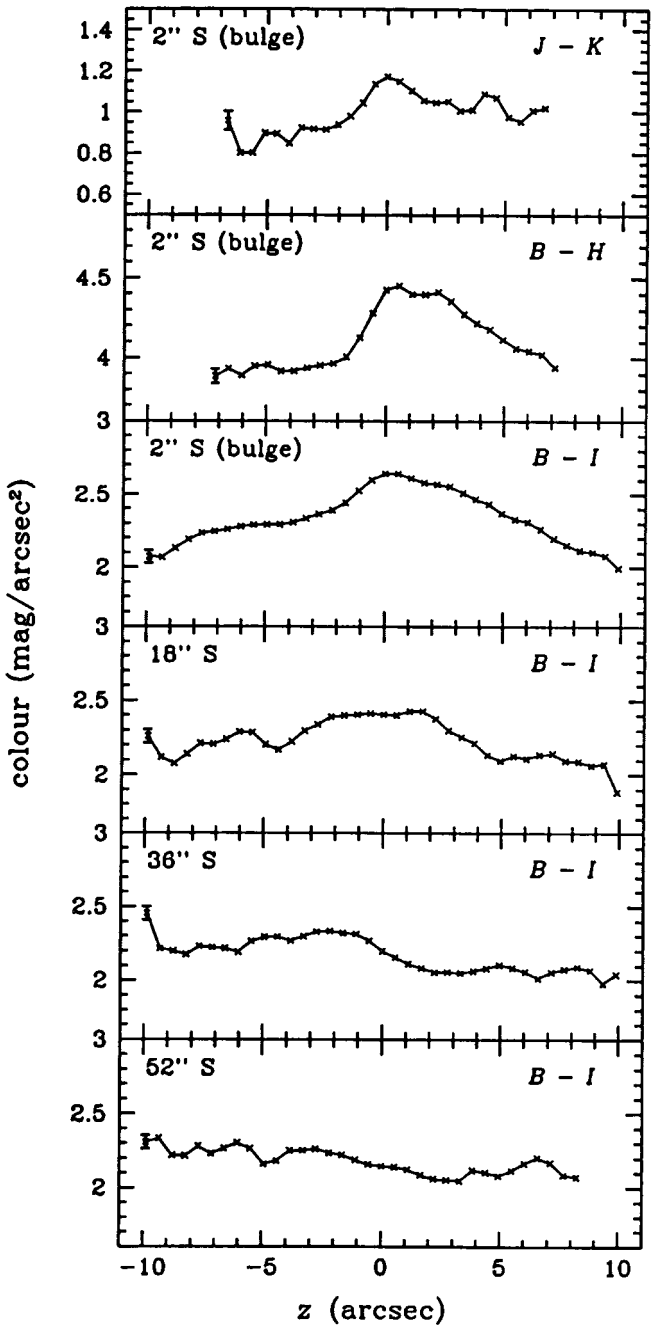

Fig. 8. Colour profiles at four positions along the major axis of NGC 6504.

5 Thick disk?

5.1 Evidence for thick disks in other (spiral) galaxies

The main reason to introduce a thick disk component in galaxies is its presence in our own Galaxy. In the solar neighbourhood it is not possible to model the vertical profile accurately without the addition of a component with a scale height of $\sim$ 1 kpc, which accounts for a few percent of the star light (Gilmore & Reid, 1983).

In external galaxies, the existence of a thick disk has not been proven unambiguously. The profiles of NGC 891 can be explained by a thick disk, but also by a "returning" bulge with axis ratios increasing towards the outer parts (van der Kruit, 1984; Bahcall & Kylafis, 1985), as discussed in Sect. 4.2. In Hamabe & Wakamatsu (1989) the excess in NGC 4762 is associated with a ring surrounding this galaxy.

Van der Kruit & Searle (1981a) analyse two systems that do not contain any significant bulge component, NGC 4244 and NGC 5907. A study of such galaxies makes the interpretation of excess light over exponential profiles in the outer parts easier, since it cannot be attributed to the bulge. In NGC 5907 van der Kruit & Searle (1981a) find an excess starting at $\mu_B = 27$ mag arcsec^{-2}, somewhat fainter than what we find here, but in NGC 4244 an exponential distribution without excess fits very well. It indicates that the thick disk in NGC 5907 is probably real, but also that not every galaxy has a thick disk.

Possibly the best detection of a thick disk is the one by van der Kruit & Searle (1981a) and Jensen & Thuan (1982) in NGC 4565. Using extremely deep photographic photometry, the latter authors were able to follow a thick disk component down to 30 B-mag arcsec^{-2}. The vertical profiles of this galaxy exhibit much similarity with those of NGC 6504. Van der Kruit & Searle (1981a) show that there is too much light in the outer parts of NGC 4565 to be explained by a $z^{\frac{1}{4}}$ bulge. Jensen & Thuan (1982) also found a young disk component similar to the one in NGC 6504. They find a scale height of the thick disk of NGC 4565 of $6.6z_0$, and a central surface brightness of 25.26 mag arcsec^{-2}. The colour index B–R is approximately 1.4.

In other publications concerning early type spirals, a thick disk has never been clearly detected.

5.2 Parameters of the thick disk; discussion

The excess in the outer regions is examined by subtracting the model from the data. At z heights greater than $20''$ the signal-to-noise ratio is too low to examine individual profiles. Supposing the scale height of the thick disk does not change significantly we constructed an average vertical profile of the entire galaxy (Fig. 9).

Again, we fitted between $|z| = 10''$ and $|z| = 16''$; in all bands the scale height is taken to be equal to the scale height in I. Table 4 contains the parameters of the fits. In Fig. 10 the residuals in the I band are plotted. The parameters of the fits to the residuals are also shown in Table 4.

The central surface brightness of the thick disk as given by the fits is 23.1 I-mag arcsec^{-2}. The average surface brightness of the thin disk is $\sim$ 18.2 I-mag arcsec^{-2} at $z = 0$, which means that the intensity of the thick disk is $\sim$ 1% of the intensity of the thin disk in the centre. The ratio of the scale heights is $13''/3''.3 \approx 4$. The colour index B–$R \approx 1.4$.

These parameters agree well with those found by Jensen & Thuan (1982) for NGC 4565. The thick disk in NGC 6504 is approximately of equal B central surface brightness as the one in NGC 4565. The ratio of the scale heights of thick and thin disk is 6.6 for NGC 4565 and 4 for NGC 6504. The colour indices are equal.

Gilmore et al. (1990) show that the central surface brightness of the thick disk of the Galaxy is 1 to 5 percent of the brightness of the thin disk. The scale height of the thick disk

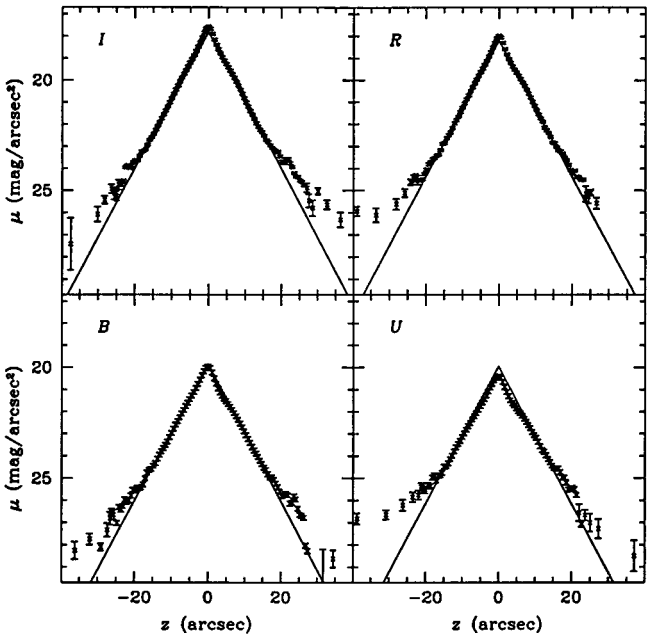

Fig. 9. Average profiles of the entire galaxy. The fit is done between 10″ and 16″.

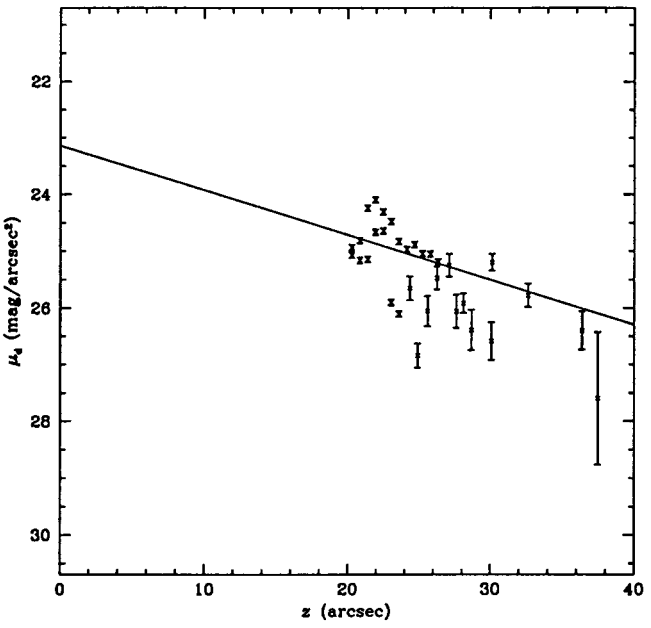

Fig. 10. Average thick disk profile in the I band.

is 3 to 4 times greater than that of the thin disk. So, the values derived here lie well within the range assumed for thick disks. We note, however, that the uncertainties in our fits are large.

6 Conclusions

We find three disk components in NGC 6504. The thin disk is easily detectable at intermediate heights: the profiles are exponential between $|z| = 10''$ and $|z| = 20''$. The scale height of the stars is independent of radius and about equal to $3''.3 = 1.1$ kpc (if NGC 6504 has an inclination not significantly different from 90° [see Sect. 4.1]). Using data in U, B, R and I we analyse the colour dependence of the profiles and find that the distribution of the stars is probably closer to a sech(z) than an exponential law.

In the central parts we find evidence for a young disk with a very small scale height. A combination of this dusty young disk, and a thin disk with a vertical distribution that is flatter than exponential in the centre, can explain the data in all bands.

There is a strong indication of the presence of a thick disk in NGC 6504. The scale height is $\sim 4z_0$ and the central surface brightness is about 1% of that of the thin disk, both similar to the values for the Galactic thick disk and that of NGC 4565.

The integration time is the limiting factor in establishing the parameters of the thick disk in this Chapter. The data are just deep enough to *detect* the thick disk and deeper data are needed to examine its properties. This study shows that the question whether thick disks exist in other galaxies may be answered on the basis of deep photometry of edge-on spirals. In a systematic study one may establish if thick disks are common and/or whether they are the result of mergers or tidal interactions, or the result of secular evolution of the thin disk.

Table 4. Parameters of fits to average profiles.

	thin disk		thick disk	
band	z_0	μ_0	z_0	μ_0
I	3.23	17.82	12.7	23.1
R	3.23	18.20	12.7	23.8
B	3.23	19.85	12.7	25.2
U	3.23	19.96	12.7	24.9

Acknowledgements. This research is based on data from the Isaac Newton Telescope at La Palma operated by the RGO at the Observatorio del Roque de los Muchachos of the Instituto de Astrofísica de Canarias. We have made use of the La Palma Archive, and the NASA/IPAC extragalactic database (NED). We thank P. van der Kruit for comments on the manuscript and the referee, M. Hamabe, for his useful suggestions.

References

Aoki, T.E., Hiromoto, N., Takami, H., Okamura, S., 1991, PASJ 43, 755
Bahcall, J.N., Kylafis, N.D., 1985, ApJ 288, 252
Balcells, M., Peletier, R.F., 1994, AJ 107, 135
Barnaby, D., Thronson, H.A. Jr., 1992, AJ 103, 41
Burstein, D., 1979, ApJ 234, 829
Carney, B., Latham, D.W., Laird, J.B., 1989, AJ 97, 423
de Grijs, R., Peletier, R.F., van der Kruit, P.C., 1997, A&A, in press **(Chapter 8)**
de Vaucouleurs, G., de Vaucouleurs, A., Corwin, H.G., Buta, R.J., Paturel, G., Fouqué, P., 1991, Third Reference Catalog of Bright Galaxies, New York: Springer **(RC3)**
Florido, E., Prieto, M., Battaner, E., Mediavilla, E., Sanchez-Saavedra, M.L., 1991, A&A 242, 301
Gilmore, G., King, I.R., van der Kruit, P.C., 1990, The Milky Way as a Galaxy, Mill Valley: University Science Books

Gilmore, G., Reid, N., 1983, MNRAS 202, 1025
Habing, H.J., 1988, A&A 200, 40
Hamabe, M., Wakamatsu, K., 1989, ApJ 339, 783
Jensen, E.B., Thuan, T.X., 1982, ApJS 50, 421
Kent, S.M., 1985, ApJS 59, 115
Kent, S.M., Dame, T.M., Fazio, G., 1991, ApJ 378, 131
Kylafis, N.D., Bahcall, J.N., 1987, ApJ 317, 637
Peletier, R.F., 1993, A&A 271, 51
Pritchet, C., 1983, AJ 88, 1476
Sandage, A., 1987, AJ 93, 610
Sandage, A., Fouts, G., 1987, AJ 93, 74
Tsikoudi, V., 1979, ApJ 234, 842
van der Kruit, P.C., 1984, A&A 140, 470
van der Kruit, P.C., 1988, A&A 192, 117
van der Kruit, P.C., Searle, L., 1981a, A&A 95, 105
van der Kruit, P.C., Searle, L., 1981b, A&A 95, 116
Wainscoat, R.J., Freeman, K.C., Hyland, A.R., 1989, ApJ 337, 163